ChemComm

Enhanced Basicity of an Electron Donor-Acceptor Complex

Journal:	*ChemComm*
Manuscript ID	CC-COM-11-2022-005985.R1
Article Type:	Communication

COMMUNICATION

Received 00th January 20xx,
Accepted 00th January 20xx

DOI: 10.1039/x0xx00000x

Enhanced Basicity of an Electron Donor-Acceptor Complex

Bernard G. Stevenson,[a] Amanada V. Prascsak,[b] Annemarie A. Lee, [a] Eric D. Talbott,[a] Lisa A. Fredin*[b] and John R. Swierk*[a]

An electron donor-acceptor (EDA) complex forms between 1,4-dicyanobenzene and N-phenylpyrrolidine, which are coupling partners for the α-aminoarylation photoredox reaction. Calculations and experiments demonstrate the EDA complex is a better base than N-phenylpyrroline. A re-analysis of the α-aminoarylation reaction suggests that the EDA complex is a proton acceptor in the reaction.

Utilizing visible light to drive synthetic reactions has steadily grown in importance.[1,2] Most recent efforts towards using visible-light photosensitization have focused on employing light absorbing photocatalysts that undergo excited state electron transfer (i.e., photoredox)[3,4] or energy transfer.[5,6] More recently, there has been significant interest in the use of electron donor-acceptor (EDA) complexes as photoactive species.[7-10] For example, Aggarwal and coworkers demonstrated that a photochemical synthesis of pinacol boronic ester can be accomplished by illuminating an EDA complex of N-hyroxyphthalimide ester and bis(catecholato)diboron.[11] Amines can act as electron donors in photochemical reactions involving EDA complexes, as demonstrated by the aminodecarboxylation of tetrachlorophthalamide esters.[12] Also, an α-aminoarylation cross-coupling between cyanoarenes and amines involving an EDA complex was recently demonstrated.[13] Finally, Molander and coworkers demonstrated the combined use of an EDA complex and nickel cocatalyst for $C(sp^3)$-$C(sp^2)$ bond formation.[14]

Recently, we explored a photoredox α-aminoarylation reaction in significant detail.[15] Through the use of transient absorption spectroscopy, we were able to measure and describe all of the individual mechanistic steps and then use that data to predict external reaction quantum yields. Comparison of predicted to measured quantum yields revealed several factors limited the quantum yield, most notably formation of a light absorbing EDA complex between the two reagents, 1-phenylpyrrolidine (NPP) and 1,4-dicyanobenezene (DCB) and the use of an insoluble, light-scattering base. During the course of the α-aminoarylation reaction, NPP is oxidized by an Ir(IV) species to generate an NPP radical cation, which is subsequently deprotonated to give a neutral radical species that functions as one of the coupling partners. Exploration of the acid-base chemistry in that reaction revealed that sodium acetate was not the initial proton acceptor in the reaction, with experiments suggesting that DCB had some role as a base. However, it was unclear how DCB could function as a base. As detailed below, we now propose that the EDA complex between DCB and NPP functions as the initial proton acceptor in the reaction.

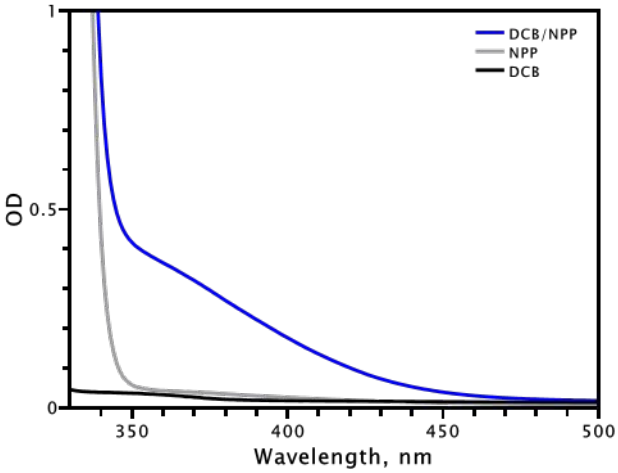

Figure 1 UV-Vis spectra of 50 mM 1,4-dicyanobenzene (DCB, black), 50 mM 1-phenylpyrrolidine (NPP, grey), and 50 mM of DCB/NPP mixture in ACN (blue).

[a] *Department of Chemistry, State University of New York Binghamton, 4400 Vestal Parkway East, Binghamton, NY 13902.*
[b] *Department of Chemistry, Lehigh University, 6 E. Packer Ave, Seeley G. Mudd, Bethlehem, PA 18015*

Electronic Supplementary Information (ESI) available: General experimental methods, NMR data for all titrations, computational methods, optimized EDA complex and $EDAH^+$ complex. See DOI: 10.1039/x0xx00000x

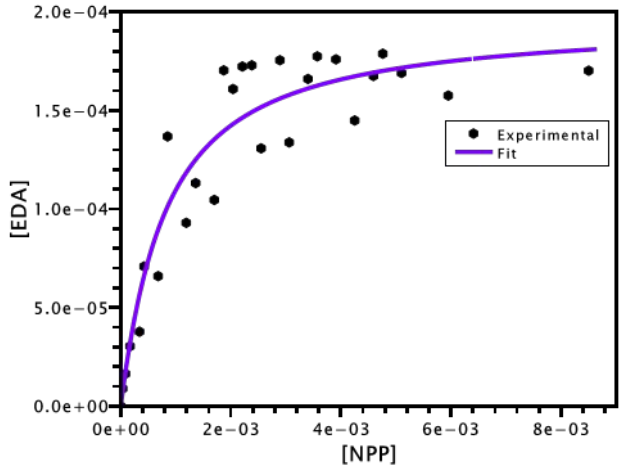

Figure 2. Experimental (black circles) equilibrium curve for formation of DCB/NPP EDA complex with varying concentrations of NPP. Purple line is fit to equation 1. The DCB 1H NMR peak shift was used as the indicator for EDA formation with ACN-d^3 as solvent.

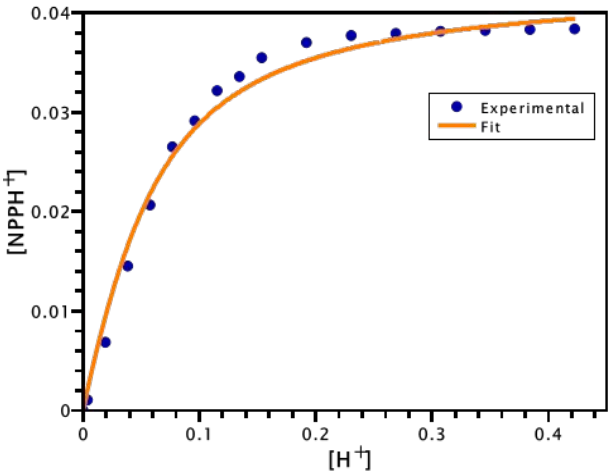

Figure 3. Experimental (blue circles) equilibrium curve for NPP with varying additions of trifluoroacetic acid. Orange line is fit to equation 1. NPP ^{1}H NMR chemical shift at δ 3.234 was used as the indicator for protonated NPP formation with ACN-d^3 as solvent.

The EDA complex of NPP and DCB exhibits a broad absorption from 350 nm to 450 nm (Figure 1), which is indicative of an EDA charge transfer band.[16] Though in our previous report we assumed that the equilibrium for the formation of the NPP/DCB EDA complex lay to the right, we did not determine an equilibrium constant for the EDA complex. We now determine the equilibrium constant and free energy of the formation for the EDA complex using ^{1}H NMR. The chemical shift of DCB (δ = 7.888 ppm, Figure S1) moves upfield with addition of NPP and was used an indicator for the EDA complex formation. Various known concentrations of NPP were added and the concentration of the EDA complex versus [NPP] was plotted and mathematically fit to determine the equilibrium constant (Figure 2). The best fit was determined by fitting the curve in Figure 2 using equation 1:

$$y = 1/2\{1/K + C + x - ((1/K + C + x)\text{^}2 - 4Cx)\text{^}1/2\} \quad \text{(eq 1)}$$

where x is the concentration of [NPP], C is the initial concentration of DCB, and y is the concentration the EDA complex.[17] The best fit of the experimental data was with K equal to 1425, which demonstrates that formation of the EDA complex is highly favourable (ΔG = -18.0 kJ/mol). This implies that under reaction conditions for the photoredox coupling, most of the DCB will be in the state of EDA complex. In the optimized DCB/NPP EDA complex, the phenyl moieties align via a π-stacking like arrangement with a packing distance of only 1.87 Å Waals (Figure S2) vs. a 3.87 Å van der Waals distance. This strong intermolecular interaction indicates a favourable formation of the EDA complex with large electronic overlap between the two molecules.

By itself, NPP is capable of functioning as a base and so the proton accepting ability was studied in the absence of DCB. Using NMR, the chemical shift of the α-amino proton (δ = 3.234 ppm, Figure S4) was monitored with the addition of trifluoroacetic acid as a proton donor (Figure 3). Equation 1 was again used to fit the data with x equal to [H^+], C equal to the initial concentration of NPP, and y equal to the concentration of [$NPPH^+$]. From the curve fit, we determined an equilibrium constant of 28.7 and ΔG of -8.3 kJ/mol, which indicates that by itself NPP will act as a proton acceptor. Computationally, the added proton on $NPPH^+$ has a typical H^+ Mulliken charge of ~0.3, while the nitrogen in NPP shows a 0.091 increase in the Mulliken charge with the addition of the proton (from -0.51 to -0.42, Figure 4).

To explore the basicity of the EDA complex, we titrated a solution of the DCB/NPP EDA complex and used the same ^{1}H NMR chemical shift at 3.234 ppm (Figure S5) to monitor the degree of protonation with added trifluoroacetic acid. The equilibrium curve was again fit to equation 1 with x equal to [H^+], C equal to the initial concentration of EDA complex, and y equal to the concentration of [$EDAH^+$]. The fit gave an equilibrium constant of 87.4 and a ΔG = -11.1 kJ/mol. (Figure 5). For the EDA complex, the equilibrium constant is more than 3 times larger than NPP alone (28.7 vs 87.4), indicating that formation of the EDA complex increases the basicity of NPP.

NMR data is consistent with the proton interacting with the nitrogen on NPP and does not indicate attachment of a proton anywhere on DCB when in the EDA complex. Specifically, we only observe a for DCB singlet that does not shift with added acid (Figure S6). Interestingly, the computationally optimized EDA complex does not show pure addition of a proton to the

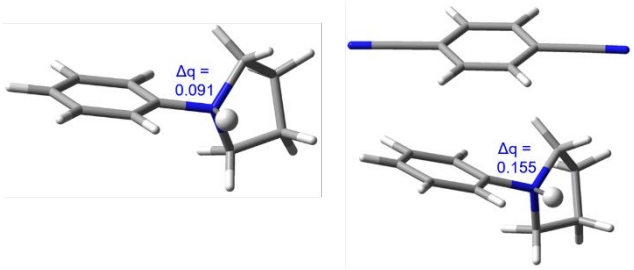

Figure 4 D3-M06-L/6-311g(d,p)/PCM(ACN) optimized $NPPH^+$ and $EDAH^+$ and the change (Δq) in Mulliken charge on each N with the addition of the proton.

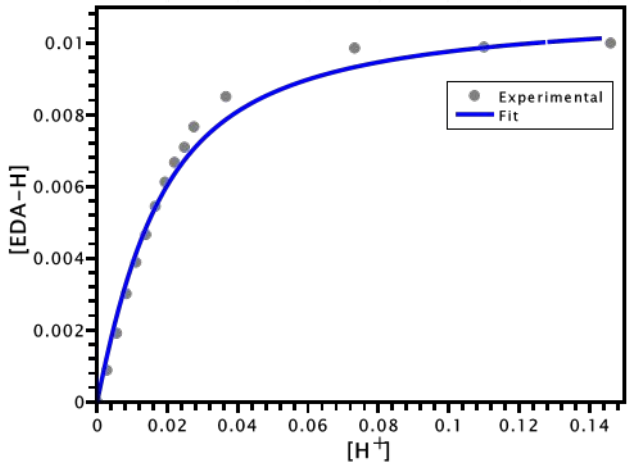

Figure 5. Experimental (gray circles) equilibrium curve for NPP/DCB EDA complex with varying additions of trifluoroacetic acid. Blue line is fit to equation 1. NPP ^{1}H NMR chemical shift at δ 3.234 was used as the indicator for protonated EDA complex formation and ACN-d^{3} was used as the solvent.

outside of the complex (i.e. to the NPP nitrogen facing away from the DCB) but instead shows that the proton is stabilized by an electrostatic interaction of the NPPH^{+} with the DCB. The packing distance increases significantly to 3.2 Å, however this is still closer than van der Waals (Figure S2) distance. This strong electrostatic stabilization leads to a more covalent N–H bond where the NPP nitrogen shows an increase in Mulliken charge of 0.155 (Figure 4, and the added proton is still ~0.3). This indicates that that the EDA complex forms a more stable conjugate base upon protonation. This is surprising as conventional wisdom suggests that nitrogen should donate electron density to DCB resulting in a decrease in Mulliken charge of the nitrogen in the EDA. In fact, computational studies of an EDA complex between 1-methylpyrrolidine and DCB indicate a Mulliken charge of -0.00149 compared to a charge of -0.437 for 1-methylpyrrolidine alone (Table S4). This suggests that in the case of the DCB/NPP EDA complex, the π-system of the phenyl ring in NPP contributes electron density to nitrogen via an inductive effect, which leads to the increase in Mulliken charge. We propose that the π-stacking of DCB and NPP increases this inductive effect, leading to the increased basicity of NPP in the EDA complex.

In our previous study, we probed the deprotonation of the NPP radical cation electrochemically.[15] It was observed that when sodium acetate was added to the reaction there was no observable difference in the rate of deprotonation. This is most likely because sodium acetate was insoluble in the solvent system for the reaction and thus proton transfer with the solid was slow. Unexpectedly, when DCB was added to the reaction mixture, without any other base, the anodic peak of NPP was pushed to more positive potentials, indicating that DCB increased the deprotonation rate of NPP$^{\bullet+}$. At the time we suggested that DCB was functioning as a base, however, given the increase in the ΔG of protonation for the EDA complex versus NPP by itself, we now suggest that the increase in the rate of deprotonation upon addition of DCB was related to the formation of the EDA complex.

Conclusions

NPP and DCB readily form an EDA complex that exhibits increased basicity relative to NPP alone. The free energy of protonation for NPP increases from -8.7 kJ/mol to -11.1 kJ/mol when in an EDA complex with DCB. Computational analysis shows that the EDA complex is formed through strong electrostatic interactions which help to stabilize the conjugate base.

This study highlights that EDA complexes can play more varied roles in photochemical reactions beyond just light absorption. The results of this study and our previous work demonstrate that in the α-aminoarylation photoredox coupling of DCB and NPP, the NPP/DCB EDA complex functions to deprotonate the NPP radical cation and then shuttle those protons to sodium acetate. In general, EDA complexes containing amines like NPP are common.[12,18-20] As we have demonstrated,[15] acid-base chemistry in photochemical reactions can be poorly described and amine-containing EDA complexes may play a role in accepting and/or shuttling protons, opening the door to unexpected pathways in the reaction. As the use of EDA complexes in photochemical transformation is further developed, an increased focus on understanding how non-photochemical properties change is required.

Conflicts of interest

There are no conflicts to declare.

Notes and references

1 S. P. Pitre, and L. E. Overman, *Chem. Rev.*, 2022, **122**, 1717-1751.
2 S. Reischauer and B. Pieber, *iScience*, 2021, **24**, 102209.
3 N. Holmberg-Douglas and D. Nicewicz, *Chem. Rev.*, 2022, **122**, 1925-2016.
4 M. Shaw, J. Twilton, and D. MacMillan, *Org. Chem.*, 2016, **81**, 6898-6926.
5 Q.-Q. Zhou, Y.-Q. Zou, L.-Q. Lu, and W.-J. Xiao, *Angew. Chem., Int. Ed.*, 2019, **58**, 1586-1604.
6 J. Gro□kopf, T. Kratz, T. Riotti, and T.Bach, *Chem. Rev.*, 2022, **122**, 1626-1653.
7 G. Crisenza, D. Mazzarella and P. Melchiorre, *J. Am. Chem. Soc.*, 2020, **142**, 5461-5476.
8 J. Wu, P. S. Grant, X. Li, A. Noble, and V. K. Aggarwal, Angew. Chem., Int. Ed,. 2019, 58, 5697-5701
9 A. Noble, R. S. Mega, D. Pasterer, E. L. Myers, and V. K. Aggarwal, *Angew. Chem., Int. Ed.*, 2018, **57**, 2155-2159.
10 B. Liu, C.-H. Lim, and G. Miyake, *J. Am. Chem. Soc.*, 2017, **139**, 13616-13619.
11 A. Fawcett, J. Pradeilles, Y. Wang, T. Mutsuga, E. L. Myers, and V. K. Aggarwal, *Science*, 2017, **357**, 283-286.
12 L. Bosque, and T. Bach, *ACS Cat.*, 2019, **9**, 9103-9109.
13 C. Xu, F. Shen, G. Feng, and J. Jin, *Org. Lett.*, 2021, **23**, 3913-3918.
14 L. Kammer, S. Badir, R. Hu, and G. Molander, Chem. Sci., 2021, 12, 5450-5457
15 B. Stevenson, E. Spielvogel, E. Loiaconi, V. Wambua, R. Nakhamiyayev, and J. Swierk, J. Am. Chem. Soc., 2021, 143, 8878-8885.

16 C. G. S. Lima, T. Lima, M. Duarte, I. D. Jurberg, and M. W. Paixão, *ACS Catal*., 2016, **6**, 1389-1407.
17 F. H. Stootman, D. M. Fisher, A. Rodger, and J. R. Aldrich-Wright, *Analyst*, 2006, **131**, 1145-1151.
18 T. Tasnim, M. Ayodele, and S. P. Pitre, J. Org. Chem., 2022, 87, 10555-10563.
19 Q. Xia, Y. Li, L. Cheng, X. Liang, C. Cao, P. Dai, H. Deng, W. Zhang, and Q. Wang, *Org. Lett.*, 2020, **22**, 9638-9643.
20 20. Q. Xia, Y. Li, X. Wang, P. Dai, H. Deng, and W.-H. Zhang, Org. Lett., 2020, 22, 7290-7294.